

Exclusive K^+ production in proton-nucleus collisions

R. Shyam*, H. Lenske, and U. Mosel

Institute für Theoretische Physik, Universität Giessen, D-35292 Giessen, Germany

(Dated: November 10, 2018)

Abstract

The exclusive K^+ meson production in a proton-nucleus collision, leading to two body final states, is investigated in a fully covariant two-nucleon model based on the effective Lagrangian picture. The explicit kaon production vertex is described via creation, propagation and decay into relevant channel of $N^*(1650)$, $N^*(1710)$ and $N^*(1720)$ intermediate baryonic states in the initial collision of the projectile nucleon with one of its target counterparts which is modeled by the one-pion exchange process. The calculated cross sections show strong sensitivity to the medium effects on pion propagator and to the final hypernuclear state excited in the reaction.

PACS numbers: 25.40.Ve, 13.75.-n, 13.75.Jz

* On leave from Saha Institute of Nuclear Physics, Calcutta, India

I. INTRODUCTION

Λ hypernuclei have been studied extensively by stopped as well as in-flight (K^- , π^-) reaction [1] and also by (π^+ , K^+) reaction [2, 3]. The kinematical properties of the (K^- , π^-) reaction allow only a small momentum transfer to the nucleus, thus there is a large probability of populating Λ -substitutional states in the residual hypernucleus. On the other hand, in the (π^+ , K^+) reaction the momentum transfer is larger than the nuclear Fermi momentum. Therefore, this reaction can populate configurations with an outer neutron hole and a Λ hyperon in a series of orbits covering all bound states. During past years data on the hypernuclear spectroscopy have been used extensively to extract information about the hyperon-nucleon interaction (which could be quite different from the nucleon-nucleon interaction) within a variety of theoretical approaches (see, e.g., [4, 5]).

Alternatively, Λ -hypernuclei can also be produced with high intensity proton beams via the $(p, K^+)_{\Lambda}B$ reaction where the hypernucleus $_{\Lambda}B$ has the same neutrons and proton numbers as the target nucleus A . First set of data for this reaction on deuterium and helium targets, have already been reported in Ref. [6]. More such measurements involving heavier targets are expected to be performed at the COSY facility of the Forschungszentrum, Jülich [7]. The states of the hypernucleus excited in the (p, K^+) reaction may have a different type of configuration as compared to those excited in the (π^+ , K^+) reaction. Thus a comparison of informations extracted from the study of two reactions is likely to lead to a better understanding of the hypernuclear structure.

Theoretical studies of the $A(p, K^+)_{\Lambda}B$ reaction are rather sparse and preliminary in nature [8, 9, 10]. They are based on two main approaches; the one-nucleon model (ONM) [Fig. 1(a)] and the two-nucleon model (TNM) [Fig. 1(b) and 1(c)]. In the ONM the incident proton first scatters from the target nucleus and emits a (off-shell) kaon and a Λ hyperon. Subsequently, the kaon rescatters into its mass shell while the hyperon gets captured into one of the (target) nuclear orbits. Thus there is only a single active nucleon (impulse approximation) which carries the entire momentum transfer to the target nucleus (about 1.0 GeV/c at the outgoing K^+ angle of 0°). This makes this model extremely sensitive to details of the bound state wave function at very large momenta where its magnitude is very small leading to quite low cross sections. In the ONM calculations of (p, K^+) and also of (p, π) reactions the distortion effects in the incident and the outgoing channels have been

found to be quite important [10, 11, 12]).

In the two-nucleon mechanism (TNM), on the other hand, the kaon production proceeds via a collision of the projectile nucleon with one of its target counterparts. This excites intermediate baryonic resonant states which decay into a kaon and a Λ hyperon. The nucleon and the hyperon are captured into the respective nuclear orbits while the kaon rescatters into its mass shell. In this picture there are altogether three active bound state baryon wave functions taking part in the reaction process allowing the large momentum transfer to be shared among three baryons. Consequently, the sensitivity of the model is shifted from high momentum parts of the bound state wave functions (not very well known) to those at relatively lower momenta where they are rather well known from $(e, e'p)$ and (γ, p) experiments and are relatively larger. This could lead to larger cross sections. Moreover, in the TNM studies of other large momentum transfer reactions like (p, π) , (γ, π) , and (γ, η) the distortion effects have been found to be less pronounced [13, 14]. This type of two-nucleon model has not yet been applied to the study the $A(p, K^+)_{\Lambda}B$ reaction.

All previous calculations [8, 9, 10] of the $A(p, K^+)_{\Lambda}B$ reaction, have been done within the non-relativistic framework. However, for processes involving momentum transfers of typically 400 MeV/c or more, a non-relativistic treatment of corresponding wave functions is questionable as the lower component of the Dirac spinor is no longer suppressed in this region (see, e.g, Ref. [15]). Furthermore, in the non-relativistic description one must resolve the ambiguities of the pion-nucleon-nucleon vertex that result from the non-relativistic reduction of the full covariant pion-nucleon-nucleon vertex (see, e.g., [13, 15, 16] for more details).

In this paper, we study the $A(p, K^+)_{\Lambda}B$ reaction within a fully covariant TNM by retaining the field theoretical structure of the interaction vertices and by treating the baryons as Dirac particles. Similar to the model used in Ref. [17] to describe the K^+ production in elementary proton-proton (pp) collisions, the initial interaction between the incoming proton and a bound nucleon of the target is described by the one pion exchange mechanism which makes the dominant contribution to the elementary $ppK^+\Lambda$ process. It should, however, be mentioned that some authors have used an alternative approach for the elementary $ppK^+\Lambda$ reaction [18, 19, 20] in which kaon exchange mechanism between the two initial state nucleons leads to the K^+ production. We have not considered this mechanism here.

In our model, the initial state interaction of the incoming proton with a bound nucleon leads to $N^*(1650)[\frac{1}{2}^-]$, $N^*(1710)[\frac{1}{2}^+]$, and $N^*(1720)[\frac{3}{2}^+]$ baryonic resonance intermediate

states which make predominant contributions to elementary $pp \rightarrow pK^+\Lambda$ cross sections in the beam energy range from near threshold to 10 GeV [17]. Terms corresponding to interference among various resonance excitations are included in the total reaction amplitude. We have ignored the diagrams of type 1(a) since contributions of such processes are expected to be very small in comparison to those of the TNM. In this first exploratory study our aim is primarily to establish the relativistic TNM mechanism for the (p, K^+) reaction. Therefore, to reduce the computational complications we have used plane waves to describe the relative motions of incoming proton and outgoing kaon.

In section II, we present the details of our formalism for calculating the amplitudes corresponding to the diagrams shown in Fig. 1b and 1c. The results of our calculations performed for the $^{40}\text{Ca}(p, K^+)^{41}_{\Lambda}\text{Ca}$ reaction are presented and discussed in section III. Summary and conclusions of our work are given in section IV.

II. FORMALISM

The effective Lagrangian for the nucleon-nucleon-pion ($NN\pi$) and N^* -nucleon-pion ($N^*N\pi$) vertices are given by

$$\mathcal{L}_{NN\pi} = -\frac{g_{NN\pi}}{2m_N} \bar{\Psi} \gamma_5 \gamma_\mu \boldsymbol{\tau} \cdot (\partial^\mu \boldsymbol{\Phi}_\pi) \Psi. \quad (1)$$

$$\mathcal{L}_{N^*_{1/2}N\pi} = -g_{N^*_{1/2}N\pi} \bar{\Psi}_{N^*_{1/2}} i\Gamma \boldsymbol{\tau} \boldsymbol{\Phi}_\pi \Psi + \text{h.c.}, \quad (2)$$

$$\mathcal{L}_{N^*_{3/2}N\pi} = \frac{g_{N^*_{3/2}N\pi}}{m_\pi} \bar{\Psi}_{N^*_{3/2}} \Gamma_\mu^{N^*} \boldsymbol{\tau} \cdot \partial^\mu \boldsymbol{\Phi}_\pi \Psi + \text{h.c.} \quad (3)$$

We have used notations and conventions of Bjorken and Drell [21]. In Eq. (1) m_N denotes the nucleon mass. The operator Γ (Γ_π) is either γ_5 (unity) or unity (γ_5) depending upon the parity of the resonance being even or odd, respectively. We have used a pseudovector (PV) coupling for the $NN\pi$ vertex and a pseudoscalar (PS) one for the $N^*_{1/2}N\pi$ vertex which provides the best description of the elementary $pp \rightarrow p\Lambda K^+$ data [17]. The effective Lagrangians for the resonance-hyperon-kaon vertices are written as

$$\mathcal{L}_{N^*_{1/2}\Lambda K^+} = -g_{N^*_{1/2}\Lambda K^+} \bar{\Psi}_{N^*_{1/2}} i\Gamma \boldsymbol{\tau} \boldsymbol{\Phi}_{K^+} \Psi + \text{h.c.} \quad (4)$$

$$\mathcal{L}_{N^*_{3/2}\Lambda K^+} = \frac{g_{N^*_{3/2}\Lambda K^+}}{m_{K^+}} \bar{\Psi}_{N^*_{3/2}} \Gamma_\mu^{N^*} \boldsymbol{\tau} \cdot \partial^\mu \boldsymbol{\Phi}_{K^+} \Psi + \text{h.c.} \quad (5)$$

The operator Γ , in Eq. (4), is defined in the same way as in Eq. (2). In Eqs. (3) and (5) $\Psi_\mu^{N^*}$ is the vector spinor for the spin- $\frac{3}{2}$ particle. Further discussions about the vertices involving

such particles are given in Refs. [17, 22]. Signs and values of various coupling constants have been taken from [17] which are shown in Table I. In Eqs. (1)-(3), the $NN\pi$, $N_{1/2}^*N\pi$ and $N_{3/2}^*N\pi$ vertices are corrected for the off-shell effects by multiplying the corresponding coupling constants by form factors of the same forms as used in Ref. [17]. The values of the cut-off parameters appearing therein are taken to be 1.2 GeV in all the cases.

The propagators for pion and spin- $\frac{1}{2}$ and spin- $\frac{3}{2}$ intermediate resonances are given by

$$D_\pi(q) = \frac{i}{q^2 - m_\pi^2 - \Pi(q)}, \quad (6)$$

$$D_{N_{1/2}^*}(p) = i \left[\frac{p_\eta \gamma^\eta + m_{N_{1/2}^*}}{p^2 - (m_{N_{1/2}^*} - i\Gamma_{N_{1/2}^*}/2)^2} \right], \quad (7)$$

$$D_{N_{3/2}^*}^{\mu\nu}(p) = -\frac{i(\not{p} + m_{N_{3/2}^*})}{p^2 - (m_{N_{3/2}^*} - i\Gamma_{N_{3/2}^*}/2)^2} \times [g^{\mu\nu} - \frac{1}{3}\gamma^\mu\gamma^\nu - \frac{2}{3m_{N_{3/2}^*}^2}p^\mu p^\nu + \frac{1}{3m_{N_{3/2}^*}^2}(p^\mu\gamma^\nu - p^\nu\gamma^\mu)]. \quad (8)$$

In Eq. (6), $\Pi(q)$ is the (complex) pion self energy which accounts for the medium effects on the propagation of the pion in the nucleus. In Eqs. (7) and (8), Γ_{N^*} is the total width of the resonance which is introduced in the denominator term to account for the finite life time of the resonances for decays into various channels. Γ_{N^*} is a function of the center of mass momentum of the decay channel, and it is taken to be the sum of the widths for pion and rho decay (the other decay channels are considered only implicitly by adding their branching ratios to that of the pion channel) [17]. The medium corrections on the intermediate resonance widths has not been included as we do not expect any major change in our results due to these effects. As is pointed out in [23], the medium correction effects on widths of the s - and p -wave resonances, which make the dominant contribution to the cross sections being investigated here, are quite small which can also be proved by following the method presented in [24]). On the other hand, any medium modification in the width of the d -wave resonance is unlikely to alter our results significantly as their contributions to the cross sections are negligibly small (see the subsequent discussions).

After having established the effective Lagrangians, coupling constants and forms of the propagators, one can write down, by following the well known Feynman rules, the amplitudes for various graphs [Figs. 1b and 1c] which can be evaluated numerically by using the techniques described in Refs. [15, 25]. While writing the amplitudes the isospin part is treated separately which gives rise to a constant factor for each graph. For example, the

amplitude for graph 1b with spin- $\frac{1}{2}$ baryonic resonance is given by,

$$\begin{aligned}
M_{1b}(N_{1/2}^*) &= C_{iso}^{1b} \left(\frac{g_{NN\pi}}{2m_N} \right) (g_{N_{1/2}^* N \pi}) (g_{N_{1/2}^* \Lambda K^+}) \bar{\psi}(p_2) \gamma_5 \gamma_\mu q^\mu \\
&\times \psi(p_1) D_\pi(q) \bar{\psi}(p_\Lambda) \gamma_5 D_{N_{1/2}^*}(p_{N^*}) \gamma_5 \\
&\times \phi_K^{(-)*}(p'_K, p_K) \psi_i^{(+)}(p'_i, p_i),
\end{aligned} \tag{9}$$

where various momenta are as defined in Fig. 1b. In addition, p_{N^*} is the momentum associated with the intermediate resonance and p_Λ is that associated with the Λ hyperon. The isospin factor C_{iso}^{1b} is unity for both the graphs 1(b) and 1(c). The functions ψ are the four component (spin space) Dirac spinor in momentum space [15, 25]. $\phi_K^{(-)*}(p'_K, p_K)$ [$\psi_i^{(+)}(p'_i, p_i)$] is the wave function for the outgoing kaon [incoming proton] with appropriate boundary conditions.

To get the T matrix of the (p, K^+) reaction, one has to integrate the amplitude corresponding to each graph over all the independent intermediate momenta subject to constraints imposed by the momentum conservation at each vertex. For instance, for the amplitude corresponding to Eq. (6) the respective T matrix is given by

$$\begin{aligned}
T_{1b}(N_{1/2}^*) &= \int \frac{d^4 p'_i}{(2\pi)^4} \int \frac{d^4 p'_K}{(2\pi)^4} \int \frac{d^4 p_\Lambda}{(2\pi)^4} \int \frac{d^4 p_2}{(2\pi)^4} \\
&\times \delta(q - p_1 + p_2) \delta(p_{N^*} - p_K - p_\Lambda) \\
&\times \delta(p_\Lambda - p'_i - q + p'_K) M_{1b}(N_{1/2}^*).
\end{aligned} \tag{10}$$

For the computation of the amplitudes we make use of the momentum space Dirac equation in an external potential field [15, 25]

$$\not{p}\psi(p) = m_N \psi(p) + F(p), \tag{11}$$

where

$$\begin{aligned}
F(p) &= \delta(p_0 - E) \left[\int d^3 p' V_s(-p') \psi(p + p') \right. \\
&\quad \left. - \gamma_0 \int d^3 p' V_v^0(-p') \psi(p + p') \right].
\end{aligned} \tag{12}$$

In Eq. (12), V_s and V_v^0 represent a scalar potential and time-like component of a vector potential in the momentum space. Using Eqs. (11)-(12) the amplitudes can be reduced to a form which is suitable for numerical computations. In this study, the incoming proton spinor $\psi_i^{(+)}(p'_i, p_i)$ and the outgoing kaon wave function $\phi_K^{(-)*}(p'_K, p_K)$ are replaced by

their plane wave counterparts. This makes redundant the integrations over variables p'_i and p'_K in Eq. (10). The final T matrix (T) is obtained by summing the transition matrices corresponding to all the graphs.

The differential cross section for the (p, K^+) reaction is given by

$$\frac{d\sigma}{d\Omega} = \frac{1}{(4\pi)^2} \frac{m_p m_A m_B}{(E_{p_i} + E_A)^2} \frac{p_K}{p_i} \sum_{m_i m_f} |T_{m_i m_f}|^2, \quad (13)$$

where E_{p_i} and E_A are the total energies of incident proton and the target nucleus, respectively while m_p , m_A and m_B are the masses of the proton, and the target and residual nuclei, respectively. The summation is carried out over initial (m_i) and final (m_f) spin states.

III. RESULTS AND DISCUSSIONS

A. The bound state spinors

We have chosen the reaction $^{40}\text{Ca}(p, K^+)^{41}_{\Lambda}\text{Ca}$ for the first numerical application of our method. The spinors for the final bound hypernuclear state (corresponding to momentum p_{Λ}) and for two intermediate nucleonic states (corresponding to momenta p_1 and p_2) have been determined by assuming them to be pure-single particle or single-hole states with the core remaining inert. The quantum numbers of the two intermediate states are taken to be the same. The spinors in the momentum space are obtained by Fourier transformation of the corresponding coordinate space spinors which are obtained by solving the Dirac equation with potential fields consisting of an attractive scalar part (V_s) and a vector part (V_v) with the Woods-Saxon geometry. With a fixed set of the geometry parameters (reduced radii r_s and r_v and diffusenesses a_s and a_v), the depths of the potentials were searched in order to reproduce the binding energies of the particular state (the corresponding values are given in Table II). The quantum numbers as well as the single baryon binding energies for final hypernuclear states have been taken from the density dependent relativistic hadron field (DDRH) theory predictions of Ref. [5], which reproduce the corresponding experimental binding energies quite well.

To have an idea of the relative strengths of the upper and lower components of the Dirac spinors as a function of the transferred momentum, we show, e.g., in Fig. 2(a) the $0p_{3/2}$ Λ hyperon spinors in momentum space for the $^{41}_{\Lambda}\text{Ca}$ hypernucleus. Similar to the observation

made in Ref. [15] for nucleon spinors, we note that only for momenta $< 1.5 \text{ fm}^{-1}$, is the lower component of the spinor substantially smaller than the upper component. In the region of momentum transfer pertinent to exclusive kaon production in proton-nucleus collisions, the magnitudes of the upper and lower components are of the same order of magnitude. This clearly demonstrates that a fully relativistic approach is essential for an accurate description of processes.

The spinors calculated in this way provide a good description of the experimental nucleon momentum distributions for various nucleon orbits as is shown in Ref. [15]. In Fig. 2(b) we show the momentum distribution of the Λ hyperon in the $0p_{3/2}$ state in ^{41}Ca . The momentum distribution is defined as $q^2[|F(q)|^2 + |G(q)|^2]$ [26]. It is clear that the momentum density of this hyperon shell is of the order of 10^0 at the momentum of $0.35 \text{ GeV}/c$ as compared to $10^{-8} - 10^{-9}$ at that of $1.0 \text{ GeV}/c$. Thus in the TNM where the sensitivity of the process is shifted to lower momentum transfers, one expects to get a larger cross section for the exclusive meson production reactions.

B. Strangeness production

A crucial quantity needed in the calculations of the Kaon production amplitude [Eq. (9)], is the pion self-energy, $\Pi(q)$, which takes into account the medium effects on the intermediate pion propagation. Since the energy and momentum carried by such a pion can be quite large (particularly at higher proton incident energies), a calculation of $\Pi(q)$ within a relativistic approach is mandatory. In our study we have adopted the approach of Ref. [27] for this purpose where contributions from the particle-hole (ph) and delta-hole (Δh) excitations are taken into account. The self-energy has been renormalized by including the short-range repulsion effects by introducing the constant Landau-Migdal parameter g' which is taken to be the same for $ph - ph$ and $\Delta h - ph$ and $\Delta h - \Delta h$ correlations which is a common choice. All the relevant formulas for this calculation are given in Ref. [15]. The parameter g' is supposed to mock up the complicated density dependent effective interaction between particles and holes in the nuclear medium. Most estimates give a value of g' between 0.5 - 0.7. Like previous studies of e.g., (p, π) [15] and $(p, p'\pi)$ [28] reactions, (p, K^+) cross sections too are expected to show sensitivity to the parameter g' .

In Fig. 3 we show, e.g., the pion self-energy calculated at zero energy ($q_0 = 0$) for several

values of g' for a Fermi momentum of 230 MeV/c. $\Pi(q)$ is real and attractive for this case. We note that for $g' = 0$ the self energies are large; their magnitude decreases with increasing value of the parameter g' . It may be remarked here that the magnitudes of self-energies as shown in Fig. 3 (with $g' = 0.5 - 0.7$) are in good agreement with those reported in Ref. [29] where calculations have been done within a relativistic mean field model.

Some remarks can already be made about the effect of the self-energy correction (to the pion propagator) on various amplitudes. For the diagramme 1(c), the energy (q_0) associated with the intermediate pion is almost equal to that of the incident proton. Therefore, in the absence of the self energy term, poles may appear in the momentum integration for this diagramme. With the inclusion of self-energy (which, in general, is complex at non-zero energies), the pole is automatically removed from the real axis and the pole integration problem disappears and the graph 1(c) becomes well behaved.

On the other hand, for the diagramme 1(b) where $q_0 \approx 0$, the self-energy is real and attractive (as can be seen from Fig. 3). This leads to a small denominator of the pion propagator leading to a consequent increase in the contribution of this graph. Indeed, for magnitudes of the self-energies $\approx (\mathbf{q}^2 + m_\pi^2)$, the integration in the T matrix of graph 1(b) may even involve poles. While the self-energy effects will give a considerable increase in the calculated cross sections, the poles in the amplitude corresponding to graph 1(b) are unphysical [30]. These poles are just the pion condensates seen in early calculations of the pion polarization potential in nuclei [31]. This effect arises because nucleon-hole and Δ -hole interactions are strongly attractive at short distances. In actual situation, one should also include the strong short-ranged repulsion which comes from the exchange of heavy mesons and other many body effects; when this is done, the spurious pole problem disappears. The distortion effects, which has not been considered here, may also "soften" the poles.

In Fig. 4, we show the kaon angular distributions corresponding to various final hypernuclear states excited in this reaction. We have taken $g' = 0.5$ throughout in this figure. In all the cases the diagram 1(b) makes a dominant contribution to the cross sections. Clearly, the cross sections are quite selective about the excited hypernuclear state, being maximum for the state of largest orbital angular momentum. This is due to the large momentum transfer involved in this reaction. It may be noted that in each case the angular distribution has a maximum around 10° and not at 0° as seen in previous non-relativistic calculations for this reaction. This is the consequence of using Dirac spinors for the bound states. There are

several maxima in the upper and lower components of the momentum space bound spinors [15] in the region of large momentum transfers. Therefore, in the kaon angular distribution the first maximum may shift to larger angles reflecting the fact that the bound state wave functions show diffractive structure at higher momentum transfers [15].

In Fig. 5, we show the dependence of our calculated cross sections on pion self-energy. It is interesting to note that this has a rather large effect. We also note a surprisingly large effect on the short range correlation (expressed schematically by the Landau- Migdal parameter g'). Similar results have also been reported in case of the (p, π) reactions. However, more definite statements about the usefulness of (p, K^+) reactions in probing the medium effects on the pion propagation in nuclei must await the inclusions of distortions in the incident and outgoing channels and exchange of heavy intermediate mesons (ρ and ω).

The relative importance of the contribution of each intermediate resonance to our reaction is shown in Fig. 5. It is clear that contributions from the $N^*(1710)$ resonance dominate the total cross section at this beam energy. We also note that the interference terms of the amplitudes corresponding to various resonances are not negligible. It should be emphasized that we have no freedom in choosing the relative signs of the interference terms. This result is similar to that observed in the study of the elementary $pp \rightarrow p\Lambda K^+$ reaction [17] at this beam energy.

The cross sections near the peak are found to be about 0.1 nb/sr for the excitation of the $^{41}_{\Lambda}\text{Ca}(0d_{3/2})$ hypernuclear state at the beam energy of 2.0 GeV. This is of the same order of magnitude as the upper limit of the experimental center of mass cross section deduced for this reaction on a ^4He target at the same beam energy [6]. Nevertheless, the short-range correlations driven by heavy meson exchange diagrams could enhance these cross sections. Also use of the bound state wave functions calculated within a microscopic theory like DDRH [5] is desirable. Although the spinors for various states calculated with our well-depth search method are in good agreement with those of the DDRH theory, the parameters of the potential well are not unique. Inclusion of these effects in our TNM model is in progress. The distortion effects in the incident and outgoing channels are also being taken into account in much the same way as it has been done in the TNM calculations of the (p, π) reaction in Ref. [25].

IV. SUMMARY AND CONCLUSIONS

In summary, we have made the first exploratory study of the $A(p, K^+)_{\Lambda}B$ reaction on a ^{40}Ca target within a fully covariant general two-nucleon mechanism where in the initial collision of the incident proton with one of the target nucleons (which is mediated by the one-pion exchange mechanism), $N^*(1710)$, $N^*(1650)$, and $N^*(1720)$ baryonic resonances are excited which subsequently propagate and decay into the relevant channels. Wave functions of baryonic bound states are obtained by solving the Dirac equation with appropriate scalar and vector potentials. We have ignored, for the time being, the distortion effects in the incident and the outgoing channels as our main aim in this paper has been to establish a realistic two nucleon model for this reaction which has not been done before.

In our model the (p, K^+) reaction proceeds predominantly via excitation of the $N^*(1710)$ resonant state at the beam energy around 2 GeV. We find that the nuclear medium corrections to the intermediate pion propagator introduce large effects on the kaon differential cross sections. There is also the sensitivity of the cross sections to the short-range correlation parameter g' in the pion self-energy. Thus, (p, K^+) reactions may provide an interesting tool to investigate the medium corrections on the pion propagation in nuclei. A useful future study would be to investigate this reaction also within an initial state kaon exchange model as it might make it possible to probe the kaon self energy in the nuclear medium. Results of such calculations together with the distortion effects will be presented elsewhere.

This work has been supported by the Forschungszentrum Jülich.

-
- [1] R. E. Chrien and C. B. Dover, *Annu. Rev. Nucl. Part. Sci.* **39**, 113 (1989); H. Kohri et al., *Phys. Rev. C* **65**, 034607 (2002) and references therein.
 - [2] P. H. Pile et al., *Phys. Rev. Lett.* **66**, 2585 (1991).
 - [3] H. Hotchi et al., *Phys. Rev. Lett.* **64**, 044302 (2001).
 - [4] E. Hiyama, M. Kamimura, T. Motoba, T. Yamada, and Y. Yamamoto, *Phys. Rev. Lett.* **85**, 270 (2000); H. Nemura, Y. Akaishi, and Y. Suzuki, *Phys. Rev. Lett.* **89**, 142504 (2002). D. Vretenar, W. Poschl, G. A. Lalazissis, and P. Ring, *Phys. Rev. C* **57**, 1060 (1998).
 - [5] C. M. Keil, F. Hofmann, and H. Lenske, *Phys. Rev. C* **61**, 064309 (2000); C. M. Keil and H. Lenske, *Phys. Rev. C* **66**, 054307 (2002).

- [6] J. Kingler et al., Nucl. Phys. **A634**, 325 (1998).
- [7] O. B. W. Schult et al., Nucl. Phys. **A585**, 247c (1995).
- [8] S. Shinmura, Y. Akaishi, and H. Tanaka, Prog. Theo. Physik **76**, 157 (1986).
- [9] V. I. Komarov, A. V. Lago, and Yu. N. Uzikov, J. Phys. G: Nucl. Part. Phys. **21**, L69 (1995);
V. N. Fetisov, Nucl. Phys. **A639**, 177c (1998).
- [10] B. V. Krippa, Z. Phys. **A 351**, (1995) 411.
- [11] D. F. Fearing and G. A. Miller, Annu. Rev. Nucl. Part. Sci. **29**, 121 (1979).
- [12] E. D. Cooper and H. S. Sherif, Phys. Rev. Lett. **47**, 818 (1982); Phys. Rev. C **25**, 3024 (1982).
- [13] P. W. F. Alons, R. D. Bent, J. S. Conte, and M. Dillig, Nucl. Phys. **A480**, 413 (1988).
- [14] W. Peters, H. Lenske, and U. Mosel, Nucl. Phys. **A640**, 89 (1998); Nucl. Phys. **A642**, 506 (1998).
- [15] R. Shyam, W. Cassing and U. Mosel, Nucl. Phys. **A586**, 557 (1995).
- [16] M. V. Barnhill III, Nucl. Phys. **A131**, 106 (1969); L. D. Miller and H. J. Weber, Phys. Lett. **64B**, 279 (1976); R. Brockmann and M. Dillig, Phys. Rev. C **15**, 361 (1977).
- [17] R. Shyam, Phys. Rev. C **60**, 055213 (1999); R. Shyam, G. Penner, and U. Mosel, Phys. Rev. C **63**, 022202(R) (2001).
- [18] N. Kaiser, Eur. Phys. J. A **5**, 105 (1999).
- [19] A. Gasparian, J. Heidenbauer, C. Hanhart, L. Kodratyuk, and J. Speth, Phys. Lett. B **480**, 273 (2000).
- [20] J. M. Laget, Phys. Lett. B **259**, 24 (1991).
- [21] J. D. Bjorken and S. D. Drell, *Relativistic Quantum Mechanics*, (McGraw-Hill, New York, 1964).
- [22] G. Penner and U. Mosel, Phys. Rev. C **66**, 055211 (2002); **66**, 055212 (2002).
- [23] C. L. Korpa and M. F. M. Lutz, nucl-th/0306063.
- [24] S. Mallik, Eur. Phys. J. C **24**, 143 (2002).
- [25] R. Shyam, A. Engel, W. Cassing, and U. Mosel, Phys. Lett. **B273**, 26 (1991).
- [26] S. Frullani and J. Mougey, Adv. Nucl. Phys. **14**, 1 (1984).
- [27] V. F. Dmitriev and Toru Suzuki, Nucl. Phys. **A438**, 697 (1985).
- [28] B.K. Jain, J. T. Londergan, and G. E. Walker, Phys. Rev. C **37**, 1564 (1988).
- [29] T. Herbert, K. Wehrberger, and F. Beck, Nucl. Phys. **A541**, 699 (1992).
- [30] T. E. O. Ericson and W. Weise, *Pions and Nuclei*, (Clarendon, Oxford, 1988).

- [31] E. Oset, H. Toki, and W. Weise, Phys. Rep. **83**, 282 (1982); G. E. Brown and W. Weise, Phys. Rep. 27, 1 (1976).

TABLE I: Coupling constants and cutoff parameters for various vertices used in the calculations.

Intermediate State	Decay channel	g	Cutoff parameter (GeV)
N	$N\pi$	12.56	1.2
$N^*(1710)$	$N\pi$	1.04	1.2
	ΛK^+	6.12	1.2
$N^*(1650)$	$N\pi$	0.81	1.2
	ΛK^+	0.76	1.2
$N^*(1720)$	$N\pi$	0.21	1.2
	ΛK^+	0.87	1.2

TABLE II: Searched depths of vector and scalar potentials and the binding energies of the Λ and nucleon bound states. In each case we have taken $r_v, r_s = 0.987$ fm and $a_v = 0.68$ fm and $a_s = 0.70$ fm.

State	Binding Energy (MeV)	V_v (MeV)	V_s (MeV)
$^{41}_{\Lambda}\text{Ca}(0s_{1/2})$	17.882	154.884	-191.215
$^{41}_{\Lambda}\text{Ca}(0p_{3/2})$	9.677	179.485	-221.587
$^{41}_{\Lambda}\text{Ca}(0p_{1/2})$	9.140	188.188	-232.331
$^{41}_{\Lambda}\text{Ca}(0d_{5/2})$	1.544	207.490	-256.160
$^{41}_{\Lambda}\text{Ca}(1s_{1/2})$	1.108	192.044	-237.091
$^{41}_{\Lambda}\text{Ca}(0d_{3/2})$	0.753	230.206	-284.205
$^{40}\text{Ca}(0d_{3/2})$	8.333	360.980	-445.660

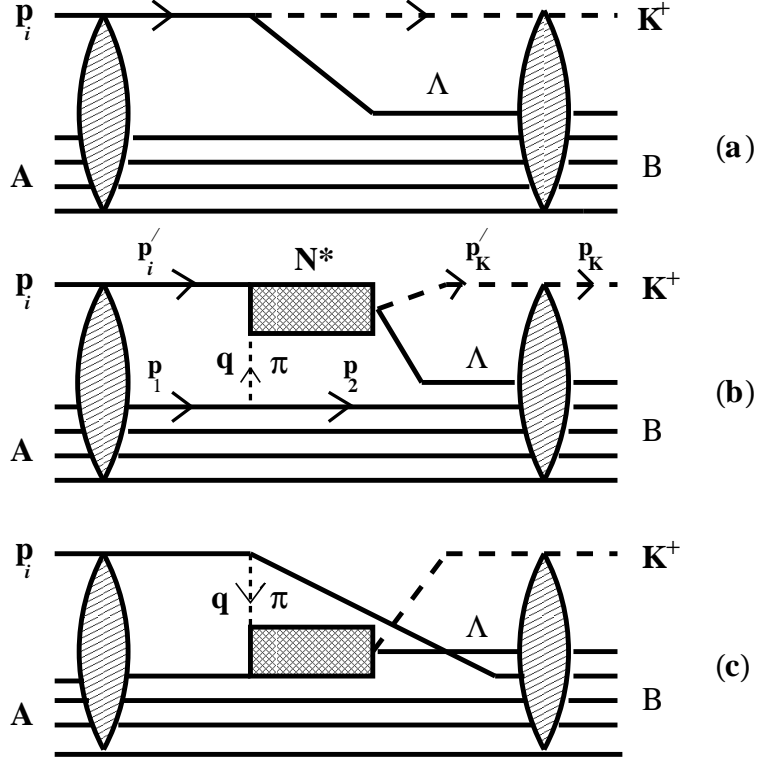


FIG. 1: Graphical representation of one- and two-nucleon models. The elliptic shaded area represent the optical model interactions in the incoming and outgoing channels.

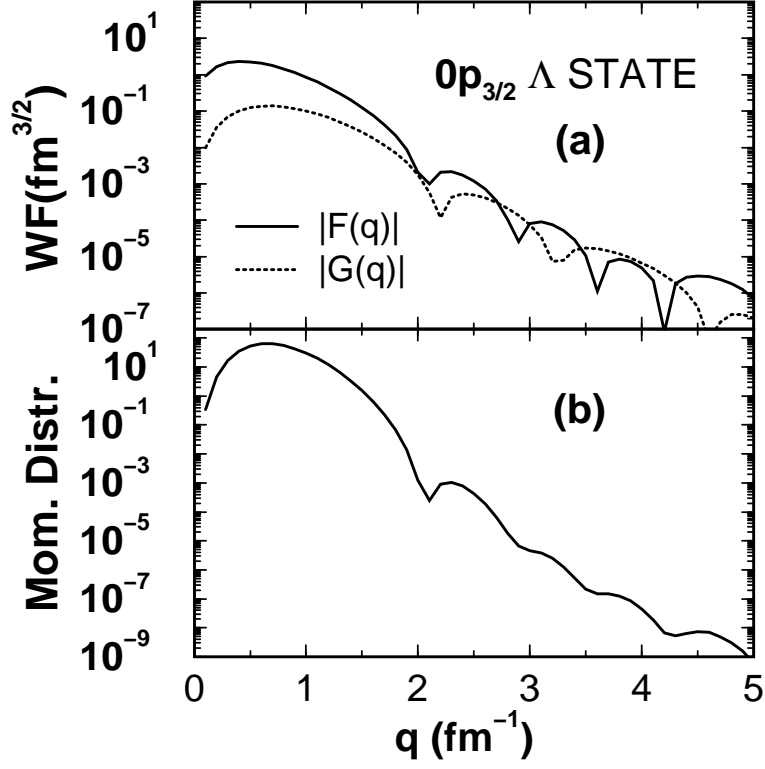


FIG. 2: (a) Momentum space spinors (WF) for $0p_{3/2} \Lambda$ orbit in $^4_{\Lambda}\text{Ca}$ hypernucleus. $|F(q)|$ and $|G(q)|$ are the upper and lower components of the spinor, respectively. (b) momentum distribution (Mom. Distr.) for the same state hyperon calculated with wave functions shown in (a).

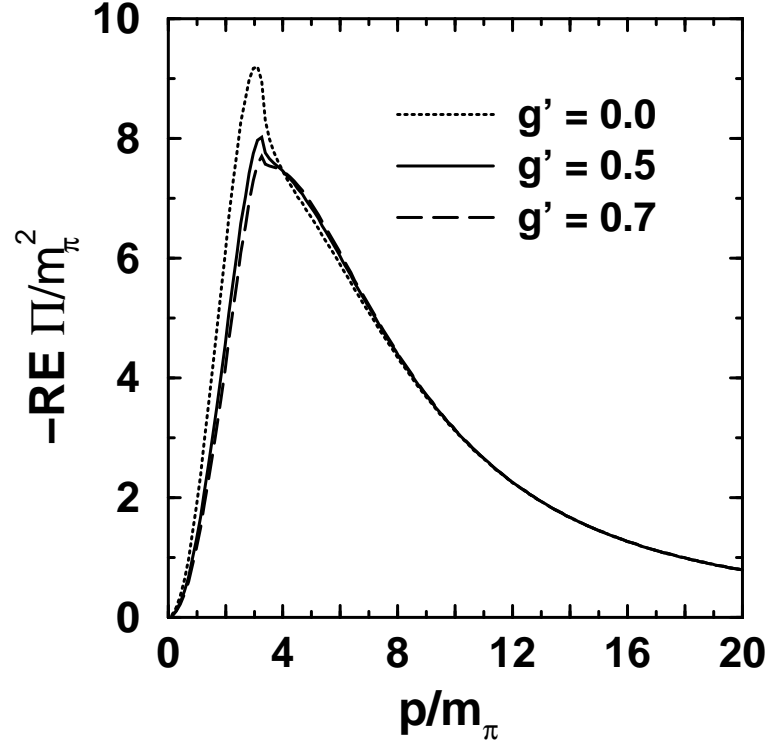


FIG. 3: Real part of the renormalized pion self energy at zero energy as a function of momentum for symmetric nuclear matter at saturation density ρ_0 . Contributions of both ph and Δh excitations are included. The results obtained with $g' = 0.0, 0.5$, and 0.7 are shown by dotted, solid and dashed lines, respectively.

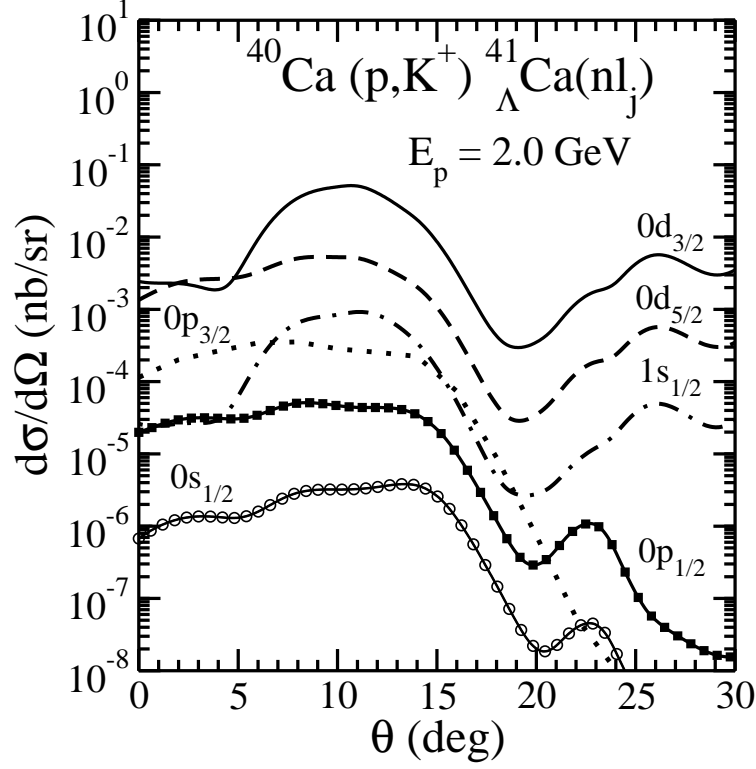


FIG. 4: Differential cross section for the $^{40}\text{Ca}(p, K^+)^{41}_{\Lambda}\text{Ca}$ reaction for the incident proton energy of 2.0 GeV for various bound states of final hypernucleus as indicated in the figure. The Λ separation energies for $0d_{3/2}$, $0d_{5/2}$, $0p_{3/2}$, $0p_{1/2}$, $1s_{1/2}$ and $0s_{1/2}$ states were taken to be 0.7529 MeV, 1.5435 MeV, 9.6768 MeV, 9.1400 MeV, 17.8820 MeV, and 1.1081 MeV, respectively. The quantum number and the binding energy of the two intermediate nucleon states were $0d_{3/2}$ and 8.3282 MeV, respectively.

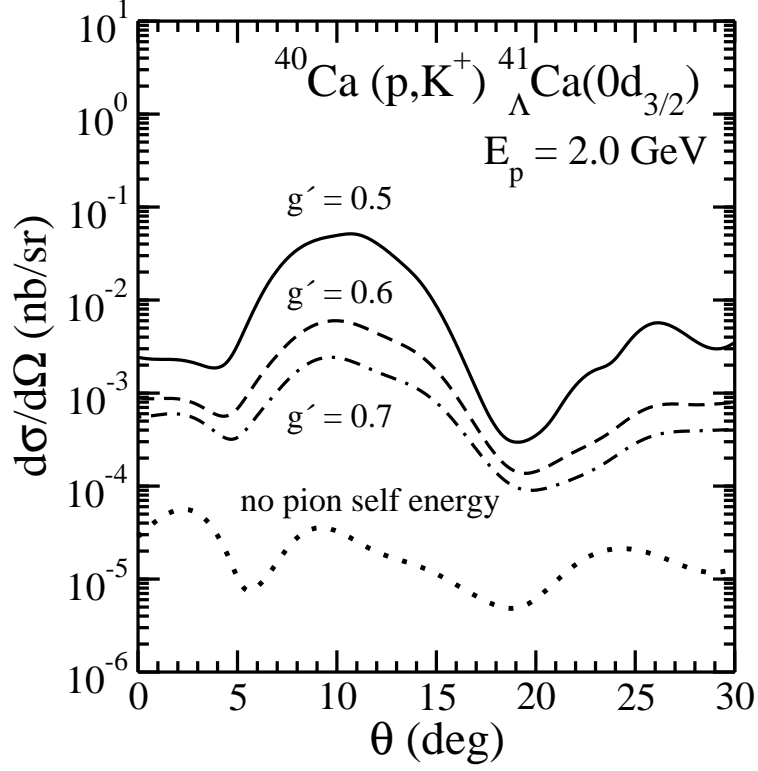


FIG. 5: Differential cross section for the $^{40}\text{Ca}(p, K^+)^{41}_{\Lambda}\text{Ca}(0d_{3/2})$ reaction for the incident proton energy of 2.0 GeV. The dotted line shows the results obtained without including the pion self-energy in the denominator of the pion propagator while full, dashed and dashed-dotted lines represent the same calculated with pion self-energy renormalized with Landau-Migdal parameter of 0.5, 0.6 and 0.7, respectively.

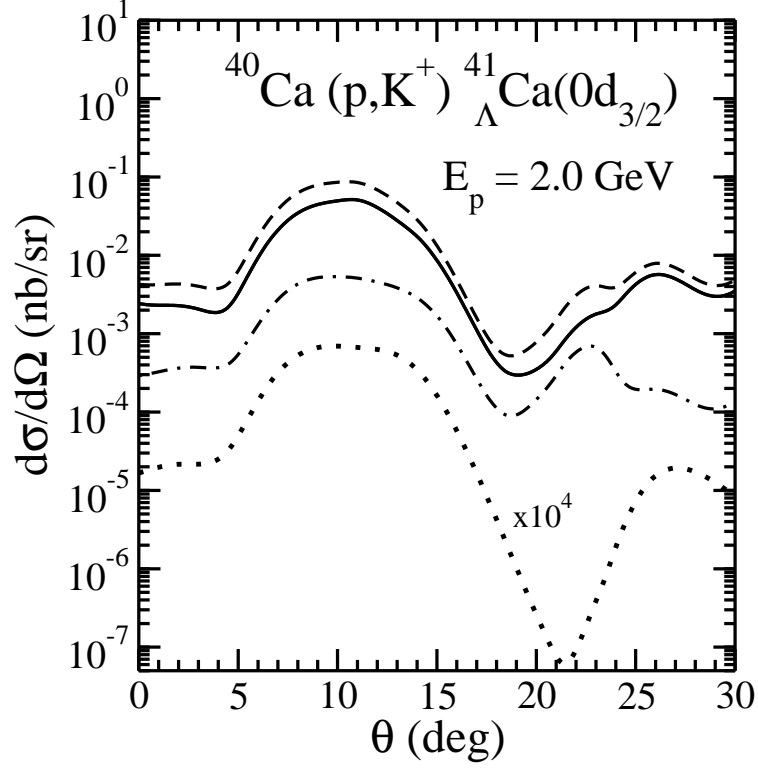


FIG. 6: Contributions of $N^*(1710)$ (dashed line), $N^*(1650)$ (dashed-dotted line) and $N^*(1720)$ (dotted line, plotted after multiplying the actual cross sections by the factor shown) to the differential cross section for the $^{40}\text{Ca}(p, K^+)^{41}_{\Lambda}\text{Ca}(0d_{3/2})$ reaction for the incident proton energy of 2.0 GeV. Their coherent sum is shown by the full line.